# Polymer Dynamics in Dilute Solutions. The Freely Rotating Chain

**Angelo Perico,* Sergio Bisio, and Carla Cuniberti**

*Centro Studi Chimico-Fisici di Macromolecole Sintetiche e Naturali, Consiglio Nazionale delle Ricerche and Istituto di Chimica Industriale, Università di Genova, Corso Europa 30, Genova, Italy.* *Received January 17, 1984*

ABSTRACT: Normal mode analysis of the Langevin dynamics of the freely rotating chain in the optimized Rouse–Zimm approximation of Bixon and Zwanzig is presented. The relaxation rates and transformation matrices in partial draining conditions are calculated by a perturbative approach starting from the results in the free draining limit. Results for the whole relaxation spectrum and intrinsic viscosity as a function of the stiffness parameter and of the hydrodynamic interaction strength are discussed in detail.

## I. Introduction

The long-range dynamics of a polymer chain in dilute Θ solution is well accounted for by a semimacroscopic approach with the solvent described as a viscous continuum and the polymer as a collection of $n$ beads of friction coefficient $\zeta$. The time evolution of this polymer model is governed by the Kirkwood generalized diffusion equation[1] or by an equivalent Langevin equation.[2]

The Rouse–Zimm approximation[3,4] to the Kirkwood equation enables one to derive quantitatively viscoelstic and frictional properties of dilute solutions of flexible polymers which agree fairly well with experimental results at low frequencies.[5] The approximation involved amounts to introducing the Rouse Matrix, exact for the bead–spring Gaussian model, as the nearest-neighbor matrix and the "preaveraged" hydrodynamic interaction matrix as the full hydrodynamic interaction tensor.

Recently, Bixon[6] and Zwanzig[7] produced a noteworthy advance in polymer dynamic methods by applying linear response theory to the Kirkwood generalized diffusion equation. Via projection operator techniques they derived an equivalent equation for the time correlation function of dynamical variables, governed by a relaxation rate constant matrix and by a memory function term. The Rouse–Zimm approximation for flexible chains is found to be a first-order approximation, in the sense that corrections due to the difference between actual and Gaussian polymer distribution or to the difference between full and preaveraged hydrodynamic interaction are of second order in these differences and are included in the memory function term. Ignoring the memory function term in the relaxation equation, one obtains an optimized Rouse–Zimm theory for an arbitrary polymer model. Subsequently,[8] Bixon and Zwanzig applied the optimized Rouse–Zimm theory to stiff polymers including rigid rings, rigid rods, and freely rotating chains with variable valence angle. For the freely rotating model in the free draining limit they obtained a dispersion equation for the relaxation rate spectrum and solved it numerically for the first few lowest terms. For partial draining, a further approximation to the mean hydrodynamic interaction matrix is needed, and calculation of the first two relaxation rates was done by direct diagonalization of the relaxation rate matrix.[8,9] At low degrees of stiffness the freely rotating chain is equivalent to a Rouse chain with a renormalized segment length and a finite number of segments, but at a high degree of stiffness it presents a relaxation rate spectrum completely changed in character, reaching ultimately the rigid rod behavior.[8] In addition, if the appropriate known limit is taken, the Kratky–Porod wormlike chain is obtained. Gotlib and Svetlov[10] succeeded in giving exact equations for the free draining relaxation rates both in the discrete and continuous wormlike limit for the freely rotating chain model in the optimized Rouse–Zimm approximation.

Despite the large body of information on dynamics of stiff chains which may be derived from the freely rotating chain model in the optimized Rouse–Zimm approximation, no further calculations after the ones presented in the paper by Bixon and Zwanzig have to our knowledge been performed. Here we present some implementations of these numerical results, calculating the whole relaxation spectrum and intrinsic viscosity in free and partial draining conditions, as a function of the degree of stiffness and of the number of beads. Free draining eigenvalues and eigenvectors are calculated by direct diagonalization of the structural symmetric matrix. A fast perturbative procedure for the calculations of eigenvalues and eigenvectors in partial draining conditions starting from the results for free draining is introduced.

## II. Relaxation Spectrum in the Free Draining Limit

The freely rotating chain is a bead-type model characterized by $n$ beads of friction coefficient $\zeta$, a segment length $a$, and the stiffness parameter $g = -\cos\theta$ with $\theta$ the angle between adjacent chain segments. At fixed $n$, by increasing $g$ one may explore different degrees of stiffness, ranging from the limit of a flexible chain ($g \to 0$) to the linear rod ($g \to 1$).

The coordinate relaxation, in the approximation of zero memory function, is governed by the relaxation matrix **HA**, where **H** is the averaged hydrodynamic interaction matrix and **A** is the nearest-neighbor structural matrix, given by Bixon and Zwanzig[8] as

$$\mathbf{A} = \frac{1-g}{1+g}\mathbf{A}_R + \frac{g}{1-g^2}\mathbf{A}^2{}_R - \frac{g^2}{1-g^2}\Delta \qquad (1)$$

where $\mathbf{A}_R$ is the usual Rouse nearest-neighbor matrix and $\Delta$ is a local perturbation which becomes important only for very high stiffness.

The eigenvalues of **HA** are proportional to the relaxation rates of the model. In the free draining limit $\mathbf{H} = 1$ and the relaxation rates are simply proportional to the eigenvalues $\lambda^0{}_l$ of the symmetric matrix **A**. In this section we extend the Bixon and Zwanzig calculations to the complete set of eigenvalues and eigenvectors, $\mathbf{Q}^0$, using a standard diagonalization procedure for symmetric matrices.[11] Our calculations are performed for $n \leq 100$ in the range $0 \leq g < 1$.

For $g = 0$, the numerical procedure gives results coincident with the known exact eigenvalues and eigenvectors of the Rouse chain. For $g > 0$, the numerical procedure is checked by comparing the mean square end-to-end distance, $\langle h^2 \rangle$, calculated by $\lambda^0{}_l$ and $\mathbf{Q}^0$ with the exact

0024-9297/84/2217-2686$01.50/0 

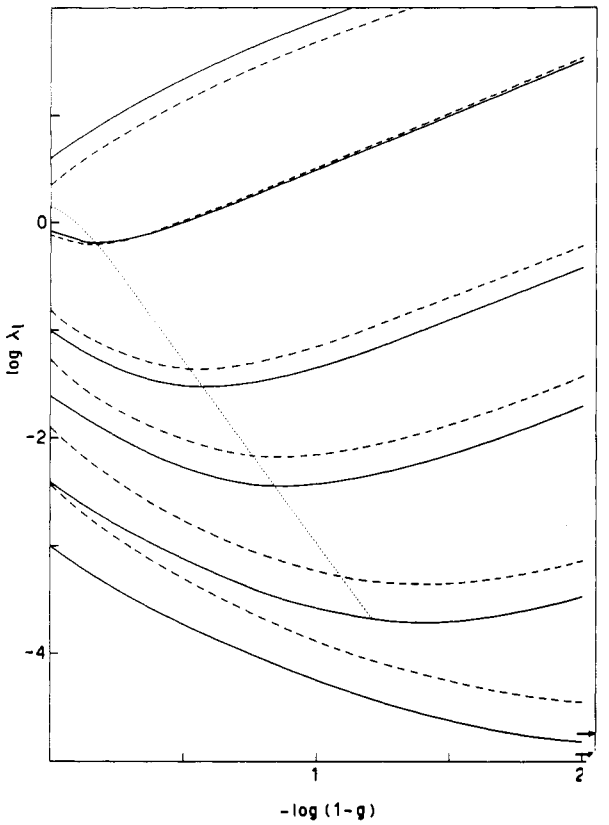


**Figure 1.** Logarithmic plot of eigenvalues against $(1-g)^{-1}$ for $n = 100$ and $l = 1, 2, 5, 10, 30$, and 99 (from bottom to top): full curves, free draining; dashed curves, partial draining; lower arrow, $\lambda^0_{rod}$ (free draining); upper arrow, $\lambda_{rod}$ (partial draining); dotted curve, locus of points of minimum from eq 3.

geometrical expression.[5] The results are coincident within the numerical accuracy.

The eigenvectors turn out to be only slightly affected by increasing the stiffness parameter $g$, but in the limit $g \to 1$, the eigenvector of the lowest mode approaches the rod value.[8]

The relaxation spectrum $\lambda^0_l$ for $n = 100$ is reported in Figure 1 as a function of $x = \log (1-g)^{-1}$. For small $l$ the same behavior shown in ref 8 is displayed. The smallest eigenvalue $\lambda^0_1$ decreases with increasing stiffness approaching asymptotically the characteristic value of the rod, $\lambda^0_{rcd} = 12/n^3$. In fact, it is easy to show from the definition of $\lambda^0_l$ as $(\mathbf{Q}^T\mathbf{A}\mathbf{Q})_{ll}$ that

$$\lambda^0_l = \frac{1-g}{1+g}\sum_i(\sum_j Q_{jl}Q^R_{ji})^2\lambda^R_i + \frac{g}{1-g^2}\sum_i(\sum_j Q_{jl}Q^R_{ji})^2(\lambda^R_i)^2 - \frac{2g^2}{1-g^2}(Q_{01}-Q_{11})^2 \quad (2)$$

with $\lambda^R_i$ and $\mathbf{Q}^R$ the Rouse eigenvalues and eigenvector matrix, respectively. For $g \to 1$, as we have pointed out above, $\mathbf{Q}_{j1}$ assumes the rod expression and we get for $l = 1$

$$\lim_{g\to 1}\lambda^0_1 = \frac{1-g}{1+g}\frac{12}{n^2} + \frac{g}{1-g^2}\frac{24}{n^3} - \frac{g^2}{1-g^2}\frac{24}{n^3} = \frac{12}{n^3} = \lambda^0_{rcd}$$

Note that if we approximate $Q_{j1} \simeq Q^R_{j1}$, the $\Delta$ contribution to $\lambda^0_1$ remains irrelevant still in the $g \to 1$ limit and $\lambda^0_1$ diverges like the higher eigenvalues. Actually the whole set of unperturbed ($\Delta = 0$) eigenvalues diverges in the rigid limit.[8]

In contrast to the behavior of $\lambda^0_1$, the eigenvalues of higher modes show a minimum at $x$ values decreasing with increasing mode number; and for high enough $l$ the eigenvalues continuously *increase* in the whole range of $x$.

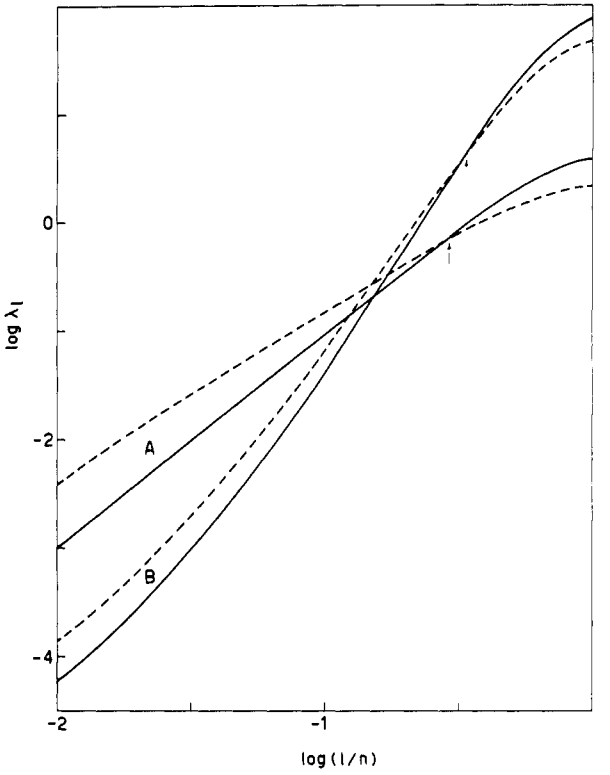


**Figure 2.** Logarithmic plot of eigenvalues against the normalized mode number for $g = 0$ (A) and $g = 0.9$ (B): full curves, free draining; dashed curves, partial draining; arrows, crossing points between regions showing opposite effects of hydrodynamic interaction on $\lambda_l$.

An approximate analytical expression for the minimum value $g_m$ of $g$ is obtained by taking for the structural matrix the "unperturbed" approximation: $\Delta = 0$. This leads to

$$g_m = \left\{-1 + \left[1 - \left(2\sin^2\frac{\pi l}{2n} - 1\right)^2\right]^{1/2}\right\} \Big/ \left(2\sin^2\frac{\pi l}{2n} - 1\right) \quad (3)$$

In Figure 1 the $g_m$ values calculated for the appropriate $l$ are connected by a dotted line. These values turn out to be a good approximation to the exact numerical results for $l > 2$. We observe that $g_m$ becomes zero for $l > n/2$.

The stiffness effect on the whole rate spectrum is better appreciated by plotting the eigenvalues $\lambda^0_l$ against the normalized mode number $l/n$ at fixed $g$. In Figure 2 the behavior at $g = 0.9$ is compared with the Rouse flexible limit $g = 0$. This kind of plot is $n$-independent for $n \geq 50$ and describes the overall stiffness dependence of the relaxation rates: increasing chain stiffness gives rise to a reduction of the lower rates but to an enhancement of the higher ones.

## III. Relaxation Spectrum in Partial Draining Conditions

As is well-known, the averaged hydrodynamic interaction matrix $\mathbf{H}$ is given in terms of the reciprocal interbead distances $R_{ij}^{-1}$ as [5]

$$H_{ij} = \delta_{ij} + \zeta_r\langle a/R_{ij}\rangle(1-\delta_{ij}) \quad (4)$$

with $\zeta_r$ the reduced bead friction coefficient

$$\zeta_r = \zeta/(6\pi\eta_0 a) \quad (5)$$

and $\eta_0$ the solvent viscosity.

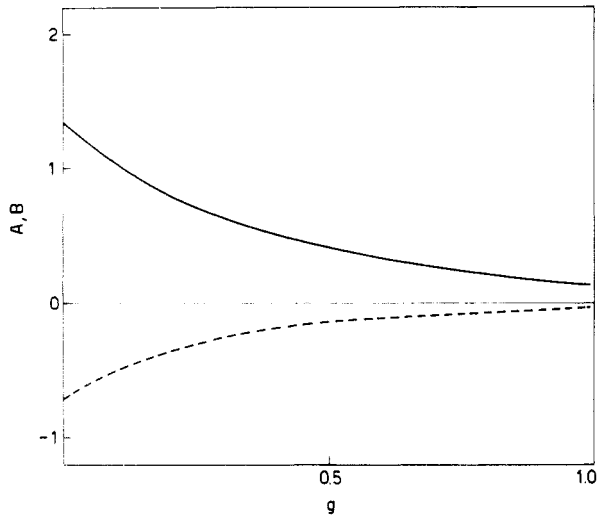


**Figure 3.** $g$ dependence of the coefficient of the quadratic and cubic terms of eq 6: full curve, A; dashed curve, B.

For a semiflexible chain the necessary average $\langle 1/R_{ij} \rangle$ may be approximately evaluated with the formula of Hearst and Stockmayer.[12] This approximation uses different distributions for large and small intersegmental distances in the wormlike chain; $\langle 1/R_{ij} \rangle$ is evaluated for intersegment distances much greater than the persistence length by a first-order Daniels distribution, and for smaller intersegment distances, a cubic approximation is used in order to introduce flexibility effects:

$$\langle 1/R_{ij} \rangle = (a|i-j|)^{-1}(1 + \alpha/3 + A\alpha^2 + B\alpha^3) \quad (6)$$

with $\alpha = L/2P$, the contour length $L = a|i-j|$, and $P$ the persistence length. Equation 6 for $\alpha = 0$ describes the hydrodynamic interaction for a rod; the term $\alpha/3$ is the correction for a weakly bending rod, while the coefficients of the quadratic and cubic terms, $A$ and $B$, were determined by imposing the Daniels and cubic approximations to have the same first and second derivatives at the intersection point.[12] The extension to the freely rotating chain may accordingly proceed by using eq 6 for the short distances and the renormalized Gaussian distribution

$$\langle 1/R_{ij} \rangle = (6/\pi)^{1/2}/(b|i-j|^{1/2}) \quad (7)$$

for the large ones. In fact, we are interested in stiffness effects relative to the freely rotating chain and not in the flexible wormlike model. The renormalized segment length $b$ and the parameter $\alpha$ are given for the freely rotating model by

$$b = a[(1+g)/(1-g)]^{1/2} \quad (8)$$

$$\alpha = |i-j|(1-g)/2 \quad (9)$$

The intersection of curve 7 with curve 6 falls at a value of $|i-j|$, $N^*$, which is an increasing function of the stiffness parameter $g$.

The correction by the cubic equation to the renormalized inverse distance is limited to a few beads at small $g$ but rapidly increases at larger $g$. As shown in Figure 3 the coefficients $A$ and $B$ result positive and negative respectively and in the stiff limit ($g \to 1$) approach approximately the values 0.118 and −0.026 obtained for the wormlike chain.[12] The small difference is due to the use of the renormalized Gaussian expression instead of the Daniels one.

The product matrix **HA** is nonsymmetric and is diagonalized to obtain the partial draining eigenvalues $\lambda_l$ as a function of $g$ and $\zeta_r$ by the perturbative approach[11] outlined in the following.

Take the eigenvectors in partial draining conditions, matrix **Q**, as a linear combination of the free draining ones, matrix $\mathbf{Q}^0$:

$$\mathbf{Q} = \mathbf{Q}^0\mathbf{B} \quad (10)$$

Define the nonsymmetric quasi-diagonal matrix

$$\mathbf{G} = (\mathbf{Q}^0)^T\mathbf{H}\mathbf{A}\mathbf{Q}^0 \quad (11)$$

Then the eigenvalue equation $\mathbf{Q}^{-1}\mathbf{H}\mathbf{A}\mathbf{Q} = \Lambda$ becomes

$$\mathbf{G}\mathbf{B} = \mathbf{B}\Lambda \quad (12)$$

This equation is solved by taking the off-diagonal elements of **G** as perturbations of the diagonal ones. The calculations here presented refer to $\zeta_r = 0.25$, since this value of the reduced friction coefficient affords the closest description of the hydrodynamic behavior of the flexible chain.[11] As we may expect a smaller $\zeta_r$ for stiffer polymers, the comparison of the results for $\zeta_r = 0.25$ with the free draining ones presented in section II will enable us to encompass the whole range of hydrodynamic interaction effects in semiflexible chains.

For $g = 0$ the perturbative procedure reproduces exactly the partial draining results for the Zimm model.[11,13]

The eigenvectors **Q** and the diagonal elements $\mu_l = (\mathbf{Q}^T\mathbf{A}\mathbf{Q})_{ll}$ turn out to be very similar to the free draining eigenvectors and eigenvalues at the corresponding $g$. Therefore, for semiflexible polymers with hydrodynamic interaction the $\mu_l$ and the **Q** may be well approximated by the free draining eigenvalues and eigenvectors, respectively, a computationally convenient result for the calculation of dynamical properties which depend on $\mu_l$ and **Q**.

The effect of the hydrodynamic interaction of the $g$ dependence of the eigenvalues is shown by the dashed curves in Figure 1 for comparison with the free draining results: the lower eigenvalues are enhanced and the higher ones depressed, the overall behavior as a function of $x$ remaining almost unchanged. As in the free draining case, $\lambda_1$ converges, although more slowly, to the rod value

$$\lambda_{rod} = \frac{12}{n^3}\left[1 + 2\zeta_r\left(\ln\frac{n}{2} - 2.68\right)\right] \quad (13)$$

calculated in the partial draining optimized Rouse–Zimm approximation. As noted by Bixon and Zwanzig, the nondraining limit of eq 13 gives a relaxation rate different for only a factor of 16/15 from the exact value. Therefore the matrix calculations for the freely rotating chain model afford a description of the chain stiffness still valid in the rod limit. A more detailed analysis of the opposed effects of the hydrodynamic interactions on low and high modes is given in Figure 2 in comparison with the free draining results. Flexible and semiflexible chains show the same qualitative behavior, though, quantitatively, larger hydrodynamic effects are observable at $g = 0$. At the same time, the crossing point which separates the low from the high mode behavior is shifted from $(l/n)^* \simeq 0.23$ at $g = 0$ to about 0.33 at $g = 0.9$.

Finally, the rigidity effects on the relaxation rates are larger in partial draining than in free draining conditions; for instance, the ratio $\lambda_1\ (g = 0)/\lambda_1\ (g = 0.99)$ is 106.9 and 64.6, respectively.

## IV. Intrinsic Viscosity

The results for the relaxation rates of semiflexible chains are here applied to the evaluation of the intrinsic viscosity:

$$[\eta] = \frac{N_A a^2 \zeta}{6\pi\eta_0 M_0}\left(\frac{1}{n}\sum_{l=1}^{n-1}\lambda_l^{-1}\right) \quad (14)$$

with $M_0$ the bead mass.

Typical results are shown in Figure 4, where $n^{-1}\sum_{l=1}^{n-1}\lambda_l^{-1}$ for $g = 0$, 0.6, and 0.9 is plotted against $n$ in a log–log plot

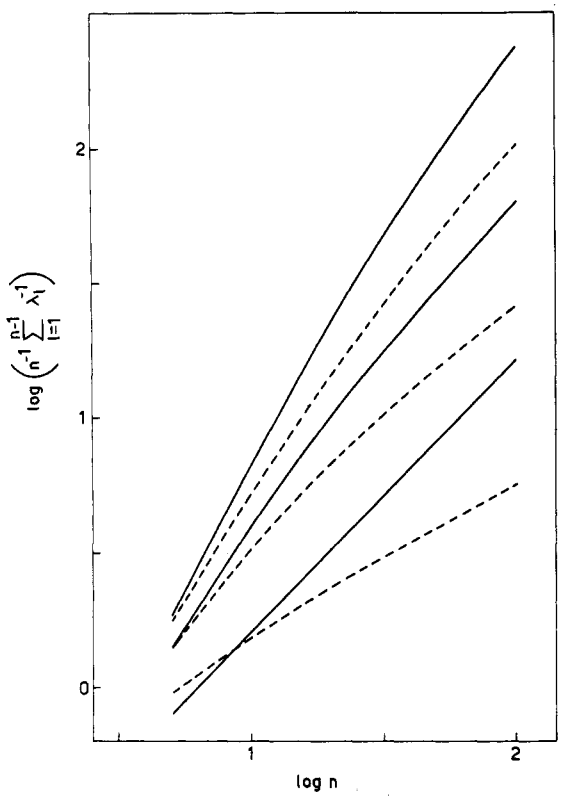


**Figure 4.** Molecular weight dependence of the intrinsic viscosity ($\propto n^{-1}\sum_{i=1}\lambda_i^{-1}$) at $g$ = 0, 0.6, and 0.9: full curves, free draining; dashed curves, partial draining.

for free and partial draining conditions. The slopes increase with increasing chain stiffness or, at fixed $g$, with decreasing $n$, in agreement with the expected behavior. The hydrodynamic interaction reduces sensibly the molecular weight dependence at any value of $g$. For instance at $n$ = 100, against the classical halving of the slope from 1 to 0.5 for the flexible chain, a reduction from about 1.8 to 1.6 is observed at $g$ = 0.99. Note that at fixed $g$ the slopes decrease with increasing $n$ toward the asymptotic limits 1 and 0.5 expected for infinitely long chains in free and partial draining, respectively. The asymptotic behavior is approached more slowly by the partial draining curves. Given the proportionality of the intrinsic viscosity to the mean square radius of gyration $\langle s^2\rangle$ in free draining and approximately to $\langle s^2\rangle R_H/n$, with $R_H$ the hydrodynamic radius, in partial draining, this result is consistent with an $R_H$ approaching its limiting value more slowly than the static $(\langle s^2\rangle)^{1/2}$.[14]

## V. Discussion

We have presented calculations for the whole relaxation spectrum and intrinsic viscosity for the optimized Rouse–Zimm approximation to the freely rotating chain model as a function of the stiffness parameter $g$. In the lower limit $g \to 0$, the calculations give the flexible Rouse–Zimm relaxation spectrum, as may be inferred from the structure of the Bixon–Zwanzig nearest-neighbor structural matrix **A**. For small stiffness and low reduced mode number $l/n$, the relaxation spectrum, both in free and partial draining conditions, may be simply described by a renormalization of the segment length. For $l/n > 0.5$ the relaxation rates increase with the stiffness parameter in the whole range. For high stiffness ($g \to 1$) all the relaxation rates but the first one become infinitely rapid, while the first one gives the rod limit, exactly in the free draining limit and with a very good approximation under partial draining conditions. The hydrodynamic interaction enhances the lower eigenvalues and depresses the higher ones, the overall behavior as a function of $g$ remaining almost unchanged.

In conclusion, our numerical calculations of the whole spectrum have shown that the optimized Rouse–Zimm approximation to the freely rotating chain describes fairly well the relaxation spectrum dependence on stiffness from the flexible to the rod limits. This spectrum and the relative transformation matrices may be used to derive dynamic properties like time-correlation functions of the bead coordinates, the sink autocorrelation function in the theory of intramolecular diffusion-controlled reactions,[15] etc., besides the intrinsic viscosity here presented. No quantitative interpretation of experimental dynamical properties of stiff polymers in terms of the model parameters has been attempted, our aim being at this stage to exploit the possibilities of the optimized Rouse–Zimm theory. The work can be extended to other bead-type polymer models. It would be of interest to make analogous calculations for the wormlike chain.

## References and Notes

(1) Kirkwood, J. G. *Recl. Trav. Chim. Pays-Bas* **1949**, *68*, 648.
(2) Zwanzig, R. *Adv. Chem. Phys.* **1969**, *15*, 325.
(3) Rouse, P. E. *J. Chem. Phys.* **1953**, *21*, 1272.
(4) Zimm, B. H. *J. Chem. Phys.* **1956**, *24*, 269.
(5) Yamakawa, H. "Modern Theory of Polymer Solutions"; Harper and Row: New York, 1971.
(6) Bixon, M. *J. Chem. Phys.* **1973**, *58*, 1459.
(7) Zwanzig, R. *J. Chem. Phys.* **1974**, *60*, 2717.
(8) Bixon, M.; Zwanzig, R. *J. Chem. Phys.* **1978**, *68*, 1896.
(9) Lukach, A.; Bixon, M., private comunication.
(10) Gotlib, Yu. Ya.; Svetlov, Yu. Ye. *Vysokomol. Soedin, Ser. A* **1979**, *A21*, 1531.
(11) Perico, A.; Piaggio, P.; Cuniberti, C. *J. Chem. Phys.* **1975**, *62*, 4911.
(12) Hearst, J. E.; Stockmayer, W. H. *J. Chem. Phys.* **1962**, *37*, 1425.
(13) Lodge, A. S.; Wu, Y. J. MRC Report No. 1250, The University of Wisconsin, 1972.
(14) Weill, G.; des Cloizeaux, J. *J. Phys. (Orsay, Fr.)* **1979**, *40*, 99.
(15) Cuniberti, C.; Perico, A. *Prog. Polym. Sci.* **1984**, *10*, 271.